

# Structural and stoichiometric studies of complexes between aroma compounds and amylose. Polymorphic transitions and quantification in amorphous and crystalline areas

B. Biais, P. Le Bail \*, P. Robert, B. Pontoire, A. Buléon

*Institut National de la Recherche Agronomique, Rue de la Géraudière, BP71627, 44316 Nantes cedex 3, France*

Received 27 October 2005; received in revised form 9 March 2006; accepted 9 March 2006

Available online 4 May 2006

## Abstract

Amylose V complexes were prepared as semi-crystalline powders from aqueous solution with three different molecules: decanoic acid, hexanoic acid, and 1,5-decanolactone. Structure and stoichiometry of the resulting amylose complexes were investigated. As evidenced by Wide Angle X-ray Scattering (WAXS), the aroma compounds lead to three different types of V amylose structure similar to  $V_h$ ,  $V_{\text{butanol}}$  and  $V_{\text{isopropanol}}$ , respectively. Extraction of aroma when included between helices, induced some polymorphic transitions towards a structure with smaller unit cells (i.e., from  $V_{\text{isopropanol}}$  to  $V_{\text{butanol}}$  and from  $V_{\text{butanol}}$  to  $V_h$ ). The location of the ligand within and/or between helices was deduced. Its content in amorphous and crystalline areas was also investigated using FT-IR spectroscopy, WAXS, and mild acid hydrolysis.

© 2006 Elsevier Ltd. All rights reserved.

**Keywords:** Amylose complexes; V types; Decanoic acid; Hexanoic acid; 1,5-Decanolactone; Fourier transform-infrared spectroscopy; Wide angle X-ray scattering; Acid hydrolysis; Stoichiometry; Delta decalactone

## 1. Introduction

Amylose, a linear polymer of D-glucose with principally  $\alpha(1-4)$  linkages, is well known for its ability to form semi-crystalline complexes with a number of small molecules. The resulting crystalline form is commonly called “V type”. Depending on the complexing molecules, different types of  $V_{\text{amylose}}$  have been described for linear alcohols (Brisson, Chanzy, & Winter, 1991; Buléon, Duprat, Booy, & Chanzy, 1984; Le Bail, Bizot, Pontoire, & Buléon, 1995; Whittam et al., 1989), monoacyl lipids (Godet, Bizot, & Buléon, 1995a; Godet, Tran, Delage, & Buléon, 1993), iodine (Bluhm & Zugenmaier, 1981; Yu, Houtman, & Atalla, 1996), dimethyl sulfoxide (Winter & Sarko, 1974),

potassium hydroxide (Sarko & Biloski, 1980), glycerol (Hulleman, Helbert, & Chanzy, 1996) and naphthol (Yamashita & Monobe, 1971). In V amylose structures, different types of helix with 4, 6, 7 or 8 glucosyl units per turn, with varied pitches have been described. Nevertheless, most of them are made from sixfold or, to a lesser extent, eightfold left-handed helices. Therefore, they can be classified in two families ( $V_6$  and  $V_8$ ) where 6 and 8 represent the number of D-glucosyl units per turn. In the  $V_6$  family, three types of crystalline packing  $V_{6I}$ ,  $V_{6II}$  and  $V_{6III}$  (where I, II and III define unit cells of different size) may be obtained depending on the nature of the complexing molecule, which can be trapped either in the single helix only ( $V_{6I}$  or  $V_h$  (Brisson et al., 1991)) or both within and between amylose helices ( $V_{6II}$  or  $V_{\text{butanol}}$  (Helbert & Chanzy, 1994) and  $V_{6III}$  or  $V_{\text{isopropanol}}$  (Buléon, Delage, Brisson, & Chanzy, 1990)). Moreover, in the  $V_8$  family, the helical cavity is larger, which allows the inclusion of bulky molecules (Yamashita & Monobe, 1971).

\* Corresponding author. Tel.: +33 2 40 67 50 54; fax: +33 2 40 67 50 84.

E-mail addresses: [bbiais@nantes.inra.fr](mailto:bbiais@nantes.inra.fr) (B. Biais), [lebaill@nantes.inra.fr](mailto:lebaill@nantes.inra.fr) (P. Le Bail), [robert@nantes.inra.fr](mailto:robert@nantes.inra.fr) (P. Robert), [pontoire@nantes.inra.fr](mailto:pontoire@nantes.inra.fr) (B. Pontoire), [buleon@nantes.inra.fr](mailto:buleon@nantes.inra.fr) (A. Buléon).

During cooking or baking processes, starch granules swell and amylose is leached out of the swollen starch granules. Some small molecules (aroma compounds or fatty acids) may then form amylose complexes (Fanta, Shogren, & Salch, 1999). Amylose complexes with aroma compounds have been studied by several authors (Heinemann, Escher, & Conde-Petit, 2003; Nuessli, Putaux, Le Bail, & Buléon, 2003; Nuessli, Sigg, Conde-Petit, & Escher, 1997; Rutschmann & Solms, 1990a) in order to determine the impact of these interactions on aroma perception in real foodstuffs (Arvisenet, Le Bail, Voilley, & Cayot, 2002; Heinemann, Conde-Petit, Nuessli, & Escher, 2001; Nuessli et al., 1997).

Crystalline structure and thermostability of amylose complexes are most often studied using X-Ray Scattering and Differential Scanning Calorimetry. They have also been studied by solid state NMR (Le Bail, Rondeau, & Buléon, 2005) or FT-IR and Raman spectroscopy (Cael, Koenig, & Blackwell, 1975). The stoichiometry of amylose complexes has been previously studied in amylose–fatty acids complexes (Fanta et al., 1999; Godet, Tran, Colonna, Buléon, & Pezolet, 1995b; Karkalas & Raphaelides, 1986), and on potato starch complexes with a number of molecules (Rutschmann, Heiniger, Pliska, & Solms, 1989; Rutschmann & Solms, 1990b, 1990c). These studies were carried out without investigation of the crystalline structure of the complexes. This point was discussed by Rutschmann and Solms (1990d) assuming that amorphous areas were comparable in length to the helices in crystalline domains. Recently, Wulff, Avgenaki, and Guzmán (2005) studied the stoichiometry of soluble complexes between substituted amylose and a number of molecules using NMR liquid spectroscopy.

The aim of the present study was to determine the structural features, namely the crystalline type, the amount and the mobility of the ligand contained in the amorphous and crystalline regions of amylose complexes obtained with decanoic acid, hexanoic acid and 1,5-decanolactone. These molecules were chosen, from the 20 constituents of a classical mixture of aroma used in sponge-cakes, because they induce the formation of highly crystalline complexes of amylose with three different types of crystalline structures. Crystalline structure and ligand quantification were carried out using X-ray scattering and FT-IR spectroscopy respectively. Coupling these techniques with selective washing in ethanol/water mixtures and mild acid hydrolysis was used to quantify the amount of trapped ligand within the amorphous and the crystalline phases. The final stoichiometry was also determined.

## 2. Materials and experimental

### 2.1. Materials

Decanoic acid (C10), hexanoic acid (C6) and 1,5-decanolactone were purchased from Aldrich (Purity 99% or greater). Amylose from potatoes was obtained from Sigma

(refer Type III) (France). Its average degree of polymerization (DP) determined by viscosimetry (Banks & Greenwood, 1969) with a “CONTRAVES Low Shear 40” viscosimeter was around 840. Potassium bromide (KBr, I.R. grade) for I.R. experiments was obtained from Sigma Chemical Co.

### 2.2. Preparation of amylose–decanoic acid, amylose–hexanoic acid and amylose–1,5-decanolactone complexes and standard mixtures

Two hundred milligrams of amylose was dispersed in 20 mL of pure water (1% (w/w)). A nitrogen flow was passed through the samples for 10 min to prevent their oxidation. The samples were, then, heated at 160 °C in a glass tube with a screw cap for 45 min. In another tube, 1 mL of hexanoic acid, 1,5-decanolactone or decanoic acid was added to 10 mL of water and then heated and mixed at 90 °C for 10 min. Due to its solid state at room temperature, the decanoic acid was pre-heated to 40 °C. The complexing molecule dispersed in water was added to amylose solution cooled at 90 °C for 2 min and intensively shaken for 2 min. The final concentration was 3.23% (v/v) for the three aroma molecules, corresponding to a molar ratio greater than 2 mol of ligand per 1 mol of glucose unit. The mixture was then cooled at room temperature and stored for 48 h. Next, the samples were centrifuged at 20,000g for 20 min at 20 °C, and the precipitates were submitted to desorption of water by equilibration over saturated NaCl solution ( $a_w = 0.75$  at room temperature).

In order to determine the amount of ligand in amylose complexes using FT-IR, standard mixtures were prepared using six different ligand/amylose ratios (% w/w): from 2.45% to 12.50% for decanoic acid, from 2.17% to 12.66% for hexanoic acid and from 2.39% to 12.32% for 1,5-decanolactone. For each concentration triplicates were made.

### 2.3. Washing procedure

After equilibrium at  $a_w = 0.75$ , each sample was washed in order to measure the amount of uncomplexed and complexed ligand in the amorphous or crystalline phase. Five milliliters of ethanol/water mixture (50/50) was added to 100 mg of precipitate and stirred for 5 min before centrifugation for 10 min at 20,000g (20 °C). In each case, one to three washing steps were performed.

### 2.4. Measurement of amylose and water content in samples

The amount of amylose in precipitates was determined using a TECHNICON automatic analyzer (Bran Luebbe auto-analyzer 3) using orcinol–sulfuric acid reagent (Tollier & Robin, 1979). About 20 mg of complexes were dissolved in 1 mL of KOH 0.5 mol/L at 4 °C for 24 h. The resulting solution was diluted 250 times with water before analysis. Results were given in glucose equivalent. For the determination

of water content, samples were dried at 105 °C and weighed at  $\pm 0.1$  mg until the weight was constant. Water contents were determined as percentage of sample weight.

### 2.5. Acid hydrolysis of amylose complexes

Mild acid hydrolysis was performed to preferentially degrade the amorphous regions of the complexes studied. Four hundred milligrams of each complex were dispersed in 80 mL of HCl (2.2 mol/L) at a final concentration of 5 mg/mL. Samples were kept at 35 °C for 35 days and gently shaken each day for 1 min as described by Robin, Mercier, Charboniere, and Guilbot (1974). Milder conditions were used for the complexes with hexanoic acid and 1,5-decanolactone:HCl (1 mol/L) and a temperature of 25 °C.

At different time point during hydrolysis, 500  $\mu$ L of the supernatant were removed, to which 500  $\mu$ L of KOH (2.2 mol/L) were added for the analysis of glucose content. After shaking, approximately 2 mL of the suspension was taken for the determination of the degree of polymerization and the amount of ligand. They were centrifuged for 5 min at 3000 rpm. The residue was suspended in 2 mL of pure water and then centrifuged again. It was then stored over a saturated NaCl solution ( $a_w = 0.75$ ). Total carbohydrates and reducing carbohydrates were determined by the methods of Tollier and Robin (1979) and Nelson (1944), respectively. The degree of polymerization of amylose during hydrolysis of the complexes was taken as the ratio of the total carbohydrates to the reducing carbohydrates. The amount of aroma compounds in complexes was determined following the method described in the FT-IR spectroscopy paragraph. The glucose content of the supernatant was also investigated as described previously.

### 2.6. Wide angle X-ray scattering

Wide angle X-ray scattering experiments were performed on precipitates to determine the crystalline type and the relative crystallinity. Approximately 30 mg of precipitates were sealed in a copper ring, between two scotch tape sheets to prevent any change in water content, and were examined by wide angle X-ray scattering with an Inel diffractometer (Inel, France), operating at 40 kV and 30 mA with a  $\text{CuK}_{\alpha 1}$  radiation (0.15405 nm) provided by a quartz monochromator. Data were monitored with a 120° curve detector (CPS 120 – Inel, France) for 2 h and normalized between 3° and 30° ( $2\theta$ ). The crystallinity was determined by subtracting the scattering diagram of an amorphous reference (dry extruded potato starch) with a scale factor adjusted in order to have null intensity on the basis line between the scattering peaks (Hermans & Weidinger, 1961). The method of Wakelin, Virgin, and Crystal (1959) was used for hydrolysis of the amylose decanoic acid complex to monitor the changes of relative crystallinity as a function of the reaction time. The crystalline standard used was obtained by subtracting the scattering

diagram of the amorphous reference from that of the most crystalline sample resulting from acid hydrolysis.

### 2.7. FT-IR spectroscopy

Infrared spectra were recorded using a Fourier transform infrared spectrometer Vector 22 (Bruker, France). The standard mixtures and samples were prepared as KBr pellets. For each experiment, aliquots of 2 mg were mixed with 100 mg KBr and die-cast at 300 kg/cm<sup>2</sup>. Spectra were obtained in the transmission mode between 2000 and 800 cm<sup>-1</sup> at 4 cm<sup>-1</sup> intervals. They were baseline corrected and normalized (OPUS software, v2.06).

### 2.8. Quantification of trapped molecules using FT-IR data and Principal Component Regression

The Principal Component Regression (PCR) is based on the Principal Component Analysis (PCA) and is used to highlight correlations between spectral and chemical data (i.e., amount of ligand in the complex) (Robert, Devaux, & Bertrand, 1996). A calibration set (standard mixtures) is used to build the regression model and the standard error is calculated from a validation set (triplicates). Applying PCA to the standard mixtures allows the relevant information to be obtained from infrared spectra. The first principal component reveals the main information held in the data; for example, it might correspond here to the variation of ligand content (see Section 3). For the PCR, the principal components are considered as predictors. The first principal component scores of the calibration set are used to assess the prediction equations (i.e.,  $[\text{Ligand}] = f(\text{first principal component score})$ ), while principal component scores of samples made it possible to determine the amount of ligand.

The calibration set was the standard mixtures we used for this study and the samples were the amylose complexes. Spectral data from standard mixtures and amylose complexes were analysed by applying the Principal Component Analysis (home built software, (Robert et al., 1996)) after normalization.

## 3. Results and discussion

### 3.1. Crystalline packing as a function of the ligand used

Wide angle X-ray scattering diagrams characteristic of amylose complexes prepared with decanoic acid (1a), hexanoic acid (1b) and 1,5-decanolactone (1c) are shown Fig. 1. The corresponding scattering angles and d-spacings are given in Table 1. The scattering diagram of the amylose complex obtained with decanoic acid is characteristic of the  $V_{61}$  packing with main scattering peaks at  $2\theta = 7.4^\circ$ ;  $12.9^\circ$ ,  $19.8^\circ$  and  $22.4^\circ$ . Additional peaks, at  $2\theta = 3.2^\circ$ ,  $11.6^\circ$ ,  $18.5^\circ$ ,  $21.6^\circ$  and  $28.9^\circ$ , correspond to recrystallized free decanoic acid ( $T_m = 32^\circ\text{C}$ ). The pattern and the observed d-spacings of the amylose–hexanoic acid complex are

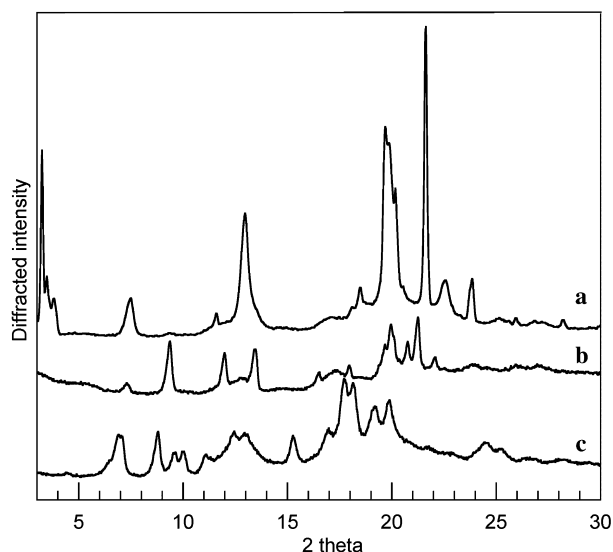


Fig. 1. X-ray scattering diagrams of amylose complexed with decanoic acid (a), hexanoic acid (b) and 1,5-decanolactone (c).

typical from the  $V_{\text{butanol}}$  packing (see Table 1) determined by Helbert and Chanzy (1994). Therefore, this complex can be classified in the  $V_{6\text{II}}$  family. The X-ray scattering diagram of the complex obtained with 1,5-decanolactone is similar to that of the amylose–isopropanol complex (Bul  on et al., 1990) ( $V_{6\text{III}}$  family, Table 1). As for hexanoic acid, no peak characteristic of free recrystallized ligand is observed. Free ligand could be present in the liquid state.

$V_{6\text{I}}$ ,  $V_{6\text{II}}$  and  $V_{6\text{III}}$  packings present the same constitutive helix with six glucosyl units per turn and similar pitch (Bul  on et al., 1990; Helbert & Chanzy, 1994). It is commonly accepted that an aliphatic chain can enter the cavity of this helix (Godet et al., 1995b). Godet et al. (1993) proposed a model of inclusion of fatty acids in which six  $\text{CH}_2$

groups of the aliphatic chain correspond to one turn of the amylose helix. It has been shown both for fatty acids and linear alcohols (Whittam et al., 1989) that retention in the amylose helix depends on the length of the aliphatic chain. Contrary to lauric (C12) acid, which is included and trapped inside the helix, caprilic (C8) acid has too short an aliphatic chain and cannot be detected in the crystalline parts. The caprilic acid is able to induce the single helical conformation but it might diffuse in the solvent after the crystallisation (Godet, 1994). Decanoic acid (C10), used in this study, has an intermediate size between the two others and therefore, is probably present within the amylose helix.

However,  $V_{6\text{I}}$ ,  $V_{6\text{II}}$  and  $V_{6\text{III}}$  packings present different unit cell parameters. Therefore, depending on the packing of helices, the unit cell parameters and the size of the complexing molecule, some space could also be available between helices for trapping. The  $V_{6\text{I}}$  structure has the smallest unit cell: orthorhombic,  $a = 1.36$  nm,  $b = 2.37$  nm,  $c = 0.8$  nm (Rappenecker & Zugenmaier, 1981) and no space available between helices for fatty acid molecules (Godet et al., 1993). The  $V_{6\text{III}}$  structure has the largest unit cell: orthorhombic,  $a = 2.82$  nm,  $b = 2.93$  nm,  $c = 0.8$  nm (Bul  on et al., 1990). The  $V_{6\text{II}}$  unit cell has intermediate dimensions: orthorhombic,  $a = 2.74$  nm,  $b = 2.65$  nm,  $c = 0.8$  nm (Helbert & Chanzy, 1994). Therefore, in complexes obtained with hexanoic acid and 1,5-decanolactone, more space is available between helices than for complexes with decanoic acid. Hexanoic acid and 1,5-decanolactone have a short aliphatic chain with five carbons, and thus might be both partially included in helix cavity and present between helices in the crystallites. Considering that hexanol (Whittam et al., 1989) and fatty acids usually form  $V_{6\text{I}}$  type with amylose, hexanoic acid, here yielding  $V_{6\text{II}}$  type, should be present between helices.

Table 1

Observed d-spacings (in nm) and corresponding Miller indexes for the three types of amylose complexed with decanoic acid, hexanoic acid and 1,5-decanolactone

Complexes with Decanoic Acid				Complexes with Hexanoic acid				Complexes with 1,5-decanolactone			
$2\theta$ (�)	d obs (nm)	h k l	d calc (nm) $V_{6\text{I}}$	$2\theta$ (�)	d obs (nm)	h k l	d calc (nm) $V_{6\text{II}}$	$2\theta$ (�)	d obs (nm)	h k l	d calc (nm) $V_{6\text{III}}$
7.4	1.190	0 2 0	1.185	7.3	1.208	2 1 0	1.217	6.9	1.278	2 1 0	1.273
		1 1 0	1.183	9.4	0.943	2 2 0	0.952	8.8	1.004	2 2 0	1.017
12.9	0.686	1 3 0	0.684	12.0	0.739	2 3 0	0.742	9.6	0.920	1 3 0	0.923
19.8	0.449	2 4 0	0.448			1 1 1	0.738	10.0	0.884	3 1 0	0.897
22.4	0.397	0 1 2	0.397	13.4	0.658	0 4 0	0.663	11.1	0.796	0 0 1	0.800
										3 2 0	0.792
3.2 <sup>a</sup>	2.741 <sup>a</sup>			16.5	0.536	3 4 0	0.537	12.5	0.710	1 4 0	0.709
11.6 <sup>a</sup>	0.760 <sup>a</sup>			18.0	0.493	3 3 1	0.497	13.0	0.683	1 2 1	0.681
18.5 <sup>a</sup>	0.478 <sup>a</sup>			20.0	0.444	3 4 1	0.445	15.2	0.580	3 4 0	0.578
21.6 <sup>a</sup>	0.417 <sup>a</sup>			20.8	0.427	5 2 1	0.428	17.0	0.522	4 1 1	0.521
28.9 <sup>a</sup>	0.309 <sup>a</sup>			21.2	0.418	4 5 0	0.419	17.7	0.500	4 2 1	0.498
				22.1	0.402	5 3 1	0.402	18.1	0.489	5 3 0	0.489
								19.2	0.462	5 0 1	0.462
								19.9	0.446	5 4 0	0.447
								24.5	0.362	5 5 1	0.363
								25.2	0.353	0 4 2	0.351

<sup>a</sup> Corresponding to free decanoic acid.



The formation of the  $V_{6II}$  packing could be due to insufficient length of the aliphatic chain and size of carboxylic group (larger than the alcohol function). 1,5-Decanolactone is still a larger molecule and its inclusion between helices induces a  $V_{6III}$  type packing.

Regarding previous studies (Godet, 1994; Godet, Bouchet, Colonna, Gallant, & Buléon, 1996), it may be assumed that the global morphology of the complexes studied here is lamellar with alternating crystalline and amorphous layers. The crystalline layer could be constituted by the packing of helices with different inter-helical volume depending on the ligand used. Amorphous layers are probably organized as a random network linking the different helices involved in the crystalline layers (Biliaderis, Page, & Maurice, 1986; Galloway, Biliaderis, & Stanley, 1989). A schematic representation of the different possible locations of trapped molecules in the crystalline parts within and between amylose helices, and in the amorphous network is given Fig. 2.

### 3.2. Measuring the total amount of ligand

In the first step, the total amount of ligand was studied without taking into account its location in amorphous or crystalline layers. Fig. 3 shows the FT-IR spectra of uncomplexed amylose (a) and amylose complexed with decanoic acid (b), hexanoic acid (c) and 1,5-decanolactone (d). The spectrum of the amylose–1,5-decanolactone complex presents an additional peak at  $1244\text{ cm}^{-1}$  corresponding to the stretching vibration of the C–O bond of the 1,5-decanolactone. As explained before, infrared spectra of standard mixtures and samples were submitted to a PCA. The first principal component explains 91%, 95% and 91% of the total variance for complexes with decanoic acid, hexanoic acid and 1,5-decanolactone, respectively. Samples are clearly all distributed along the first principal component according to the increase in trapped molecules. The spectral patterns assessed for each amylose-complex show that the first principal component has a carbonyl absorption band ( $1706\text{ cm}^{-1}$  for decanoic and hexanoic

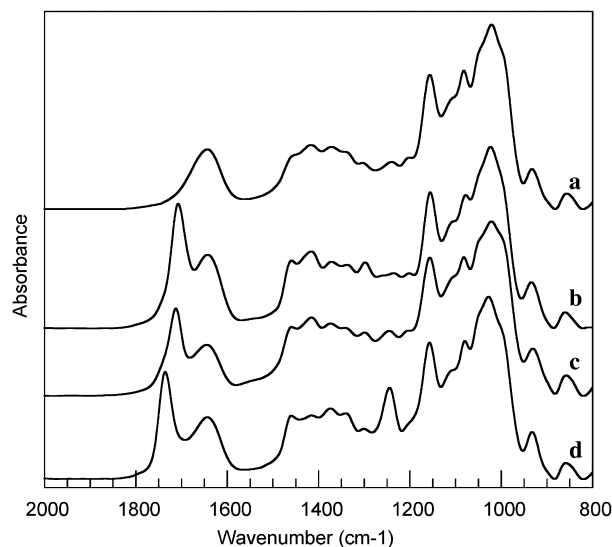


Fig. 3. FT-IR spectra of amylose (a), complexed with decanoic acid (b), with hexanoic acid (c) and with 1,5-decanolactone (d).

acid, and at  $1737\text{ cm}^{-1}$  for 1,5-decanolactone). The second principal component is essentially linked to  $1640\text{ cm}^{-1}$ , which corresponds to an absorption band of water. It takes 6%, 4% and 8%, respectively, of the total variance into account. The first principal component scores of standard mixtures and the amount of ligand are correlated, with a correlation coefficient of 0.99 for decanoic acid, 0.99 for hexanoic acid and 0.98 for 1,5-decanolactone. The assessment of prediction equations using the first principal component scores gives standard deviations of 0.7% for decanoic acid, 0.6% for hexanoic acid and 0.7% for samples with 1,5-decanolactone. The prediction equations are used to determine the amount of decanoic acid, hexanoic acid and 1,5-decanolactone within the different samples.

FT-IR results were compared with the amount of trapped ligand derived by subtraction of water and amylose contents from the total complex (Table 2). The value determined for decanoic acid (23%) is very similar to that found by FT-IR (between  $22 \pm 1.4\%$  and  $23 \pm 1.4\%$ ).

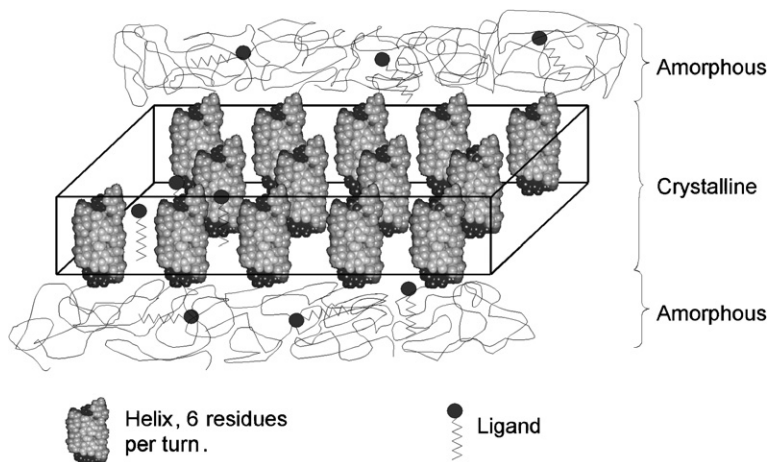


Fig. 2. Schematic representation of the structure of amylose-aroma complexes and possible location of molecules trapped.

Table 2

Measurements of amylose, ligand and water content of complexes with decanoic acid, hexanoic acid and 1,5-decanolactone

(% m/m)	Complexes with decanoic acid	Complexes with hexanoic acid	Complexes with 1,5-decanolactone
Complexes	100	100	100
Amylose content	69	69	65
Water content	8	13	11
Ligand content	23	18	24
Amount of ligand measured by FT-IR	22–23	11	16–17

Nevertheless, important discrepancies are observed in the case of hexanoic acid and 1,5-decanolactone: 18 instead of  $11 \pm 1.2\%$  (FT-IR) and 24 instead of  $16\text{--}17 \pm 1.4\%$  (FT-IR), respectively. These differences may be related to the variability of experimental conditions (sample preparation, KBr pellet, or drying process, etc.). In order to assess more precisely the amount of ligand and its location in the structure of the amylose complex, specific washing and mild acid hydrolysis treatments were combined with the FT-IR measurements.

### 3.3. Investigating the amount of free ligand by washing

Fig. 4 shows the effect of washing the amylose/decanoic acid complex in ethanol/water (50/50) mixture for 5 min on its diffraction diagram. The peaks characteristic of pure recrystallized decanoic acid at  $2\theta = 3.2^\circ$ ,  $11.6^\circ$ ,  $18.5^\circ$ ,  $21.6^\circ$  and  $28.9^\circ$  (a) disappear after the first wash (b), which shows that free decanoic acid has been removed. The diffracted intensity of  $V_{6I}$  peaks seems to decrease slightly between the first and the second wash, indicating a small loss of crystallinity and probably a slight release of includ-

ed decanoic acid. Even after two washing treatments, no transformation of the  $V_{6I}$  crystalline structure occurs. In case of the amylose/hexanoic acid complex, a progressive polymorphic transition from the  $V_{6II}$  to the  $V_{6I}$  type is observed although the presence of  $V_{6II}$  is still obvious after two washing treatments (Fig. 5). For the complex formed with 1,5-decanolactone, a transition from  $V_{6III}$  to  $V_{6II}$  type occurs during the first wash, and a partial transition to  $V_{6I}$  occurs after the second wash (Fig. 6). This type of treatment, when applied to hexanoic acid and 1,5-decanolactone amylose complexes, removed not only free ligand but also the ligand present between helices in the crystals. Therefore, it leads to a shrinkage of the  $V_{6II}$  or  $V_{6III}$  unit cell and a transition towards the more dense  $V_{6I}$  packing. Conversely, inclusion within amylose helices in the  $V_{6I}$  structure prevents decanoic acid from being extracted by the treatment. More drastic treatment involving a longer time of washing causes complete disruption of the structure and recrystallization of amylose in the B type, characteristic of retrograded amylose (Miles, Morris, Orford, & Ring, 1985).

The amount of trapped ligand varies from  $7.1 \pm 1.4\%$  (decanoic acid) to  $8.6 \pm 1.4\%$  (1,5-decanolactone) after

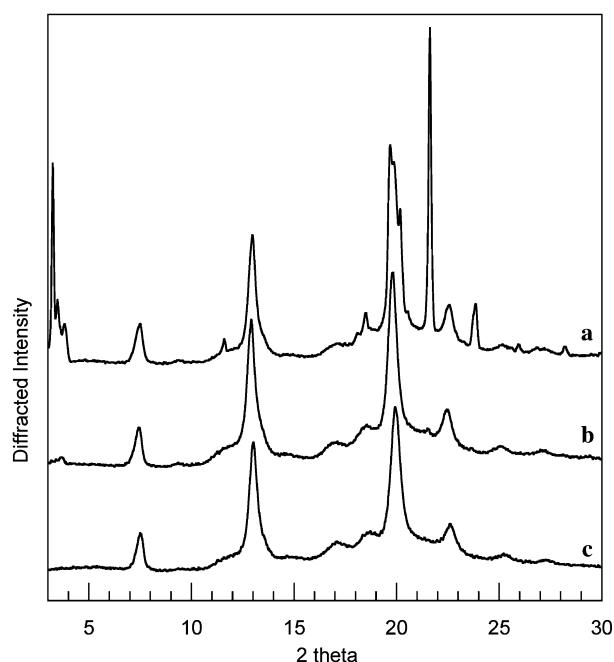


Fig. 4. X-ray scattering diagrams of amylose complexed with decanoic acid: without wash (a), after one wash (b), after two washes (c) with EtOH/H<sub>2</sub>O (50/50) for 5 min.

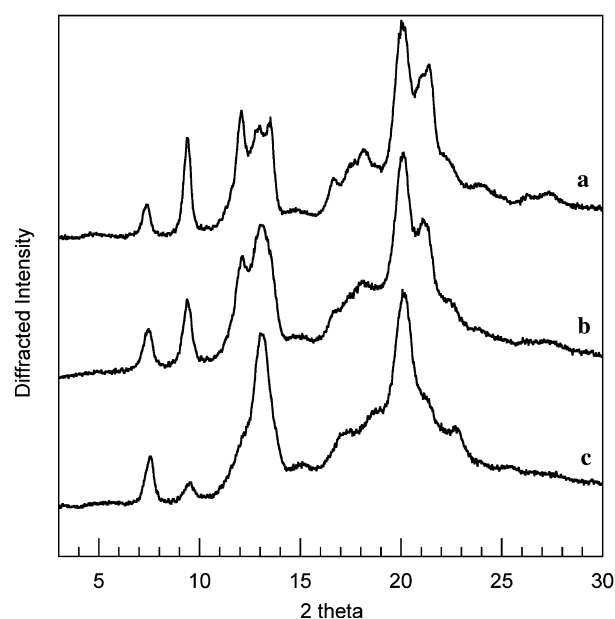


Fig. 5. X-ray scattering diagrams of amylose complexed with hexanoic acid: without wash (a), after one wash (b), after two washes (c) with EtOH/H<sub>2</sub>O (50/50) for 5 min.

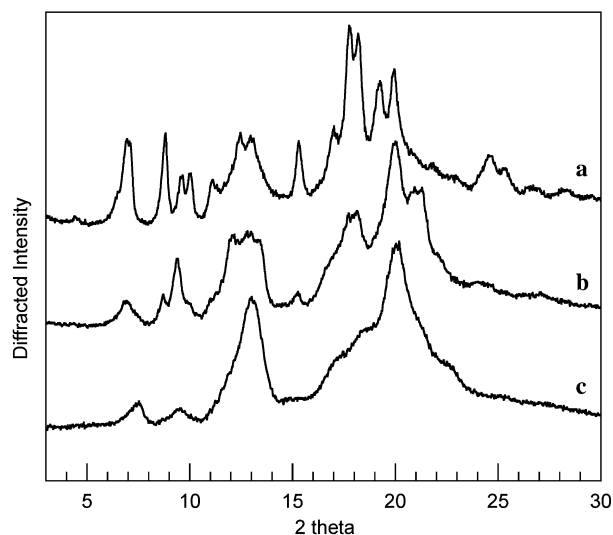


Fig. 6. X-ray scattering diagrams of amylose complexed with 1,5-decanolactone: without wash (a), after one wash (b), after two washes (c) with EtOH/H<sub>2</sub>O (50/50) for 5 min.

the first wash (Table 3) and from  $5.5 \pm 1.4\%$  (decanoic acid) to  $7.4 \pm 1.4\%$  (1,5-decanolactone) after the second data not shown. These results are in agreement with those of Wulff et al. (2005) who determined between 3.6% and 7.4% of molecules complexed with amylose, depending on the ligand used. The values found for decanoic acid are always lower, but they correspond strictly to the ligand included within helices, since there is no change in the crystalline packing after two washes. Only uncomplexed ligand is extracted and the final value (about  $5.5 \pm 1.4\%$ ) is in agreement with the work of Fanta et al. (1999), who found 5.5% and 6.8% for lauric acid and myristic acid, respectively. The amount of 1,5-decanolactone is slightly larger than that of hexanoic acid ( $8.4$  versus  $5.9\% \pm 1.2\%$ ). It could be related to the larger size of the V<sub>6III</sub> unit cell compared to the V<sub>6II</sub> one. However, it is difficult to interpret the data in detail since a mixture of V<sub>6I</sub> and V<sub>6II</sub> structures is obtained by washing.

### 3.4. Investigating the amount of ligand trapped in the crystalline domains

In order to find the amount of ligand trapped in the crystalline regions, FT-IR quantification and WAXS

experiments were combined with mild acid hydrolysis which is well known to preferentially degrade the amorphous parts in starchy samples (Robin, 1976). Fig. 7 shows the changes of crystallinity as a function of the time of hydrolysis for the amylose–decanoic acid complex. Three different phases were observed; an increase of crystallinity from  $46 \pm 5.6\%$  to  $90 \pm 5.6\%$  (Standard deviation (SD) 2.8%) during the first six/seven days, then a plateau until 27 days, and a final decrease of crystallinity. Therefore, amorphous layers are preferentially hydrolyzed during the first 6–7 days, while crystalline and amorphous regions are hydrolyzed at the same rate without any change of crystallinity for the following 20 days. The decrease of crystallinity observed after 27 days is probably induced by disruption and hydrolysis of the more resistant crystalline parts when there are no amorphous domains remaining.

The changes in the glucose content (hydrolysis rate) of the supernatant and in the amount of decanoic acid in the complex as a function of the hydrolysis time are shown in Fig. 8. The glucose content increases rapidly for 4 days and more slowly in a second stage. This confirms that during the first 4 days, easily degradable fractions associated with amorphous regions are preferentially hydrolyzed. The lower hydrolysis rate observed afterwards could correspond to more resistant amorphous or weakly crystalline domains. At the same time, the amount of decanoic acid

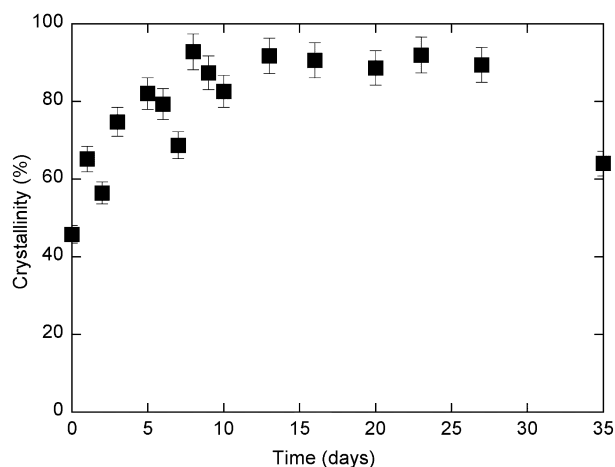


Fig. 7. Evolution of the crystallinity of the amylose–decanoic acid complex as a function of the hydrolysis time.

Table 3  
Stoichiometry of amylose complexes with decanoic acid, hexanoic acid and 1,5-decanolactone

X-ray diagram	Complexes with decanoic acid			Complexes with hexanoic acid			Complexes with 1,5-decanolactone		
	V <sub>6I</sub>			V <sub>6II</sub>			V <sub>6III</sub>		
	Not washed	Washed	Hydrolysed	Not washed	Washed	Hydrolysed	Not washed	Washed	Hydrolysed
Ligand Content	22.8 %	7.1 %	4.5 %	10.6 %	8.4 %	5.6 %	16.7 %	8.6 %	7.4%
DP	841	841	16	841	841	16 <sup>a</sup>	841	841	16 <sup>a</sup>
n <sub>ligand</sub> /n <sub>amylose</sub>	234	61	0.74	139	105	1.33	161	76	1.22
n <sub>ligand</sub> /n <sub>glucose</sub>	0.279	0.072	0.046	0.165	0.125	0.083	0.192	0.091	0.076

<sup>a</sup> Predicted DP.

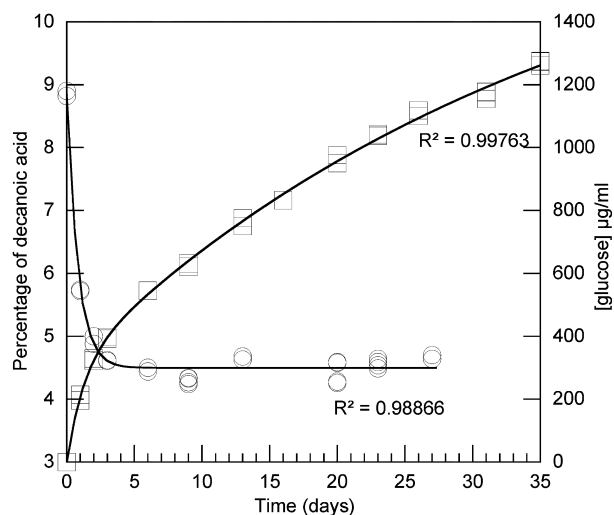


Fig. 8. Amount in percent of decanoic acid present in the complex (○) and glucose content in the medium (□) as a function of hydrolysis time for the amylose–decanoic acid complex.

in the complex decreases quickly from  $8.9 \pm 1.4\%$  to  $4.5 \pm 1.4\%$  and then reaches a plateau until the 27th day of the experiment. This rapid decrease during the first four/five days is concomitant to hydrolysis of the more easily degradable fraction. After 5 days, the amount of decanoic acid does not change while crystallinity increases for 2 days, which shows that all ligand trapped within amorphous regions is released after 4/5 days. Both ligand amount and crystallinity are then constant until 27 days, more resistant amorphous and poorly crystalline fractions being simultaneously hydrolyzed, which shows that the remaining 4.5% of decanoic acid measured by FT-IR corresponds to the ligand trapped in the more crystalline domains. The average degree of polymerization (DP) of amylose during hydrolysis also decreases very quickly in the first 3/4 days and then reaches a plateau until the last day of hydrolysis (data not shown). An average final DP of 16 (SD 4) was measured which corresponds to 2.6 helical turns.

The hydrolysis of the amylose–hexanoic acid complex in the same conditions leads to a rapid conversion from the  $V_{6II}$  to the B crystalline type in less than 4 h. It confirms the poor stability of this crystalline structure, in which the ligand is only present between helices without any strong interactions with them, as already shown by washing with ethanol/water mixtures. By using milder hydrolysis conditions (1 mol/L HCl at 25 °C), it was possible to make this conversion slower and to determine the amount of ligand present in the crystalline  $V_{6II}$  structure. In these conditions, the crystallinity decreases for the first 36 h and reaches a plateau until the end of the experiment (5 days). The percentage of hexanoic acid measured during the hydrolysis decreases from  $9.9 \pm 1.2\%$  to  $5.6 \pm 1.2\%$  and reaches a plateau after 2 days. Therefore, the later value corresponds roughly to amount of hexanoic acid in the crystalline phase. B type conversion could be due to reorga-

nization (retrogradation) of amylose fragments released by acid hydrolysis in water.

In the case of 1,5-decanolactone, a polymorphic transition from the  $V_{6III}$  to the  $V_{6II}$  type is observed without any retrogradation of amylose or crystallinity change ( $78 \pm 6\%$ ). The percentage of 1,5-decanolactone decreases from  $8.3 \pm 1.4\%$  to  $7.1 \pm 1.4\%$  and reaches a plateau. Several experiments using milder conditions for hydrolysis (acid concentration ranging from 1 to 2.2 mol/L, and temperature from 25 to 35 °C), allowed more precise determination of the amount of 1,5-decanolactone present in the  $V_{6III}$  packing just before its conversion to the  $V_{6II}$  one (data not shown). The value was found to be between  $7.8 \pm 1.4\%$  and  $7.1\%$ .

The specific behaviour of each studied sample during acid hydrolysis is related to its semi-crystalline structure. Decanoic acid is included within the amylose helix and stabilizes the helical conformation and also the  $V_{6I}$  crystalline packing, even when amylose involved in amorphous areas is hydrolysed. Hexanoic acid is only present between helices into the  $V_{6II}$  structure and apparently does not form any strong hydrogen bonds with hydroxyl groups of amylose. As soon as the amylose fragments involved in the crystalline domains are released by hydrolysis of surrounding amorphous domains, they rearrange into the B type. 1,5-Decanolactone has an intermediate behaviour, being probably partially included within the amylose helix to maintain the single helical conformation and more strongly bound when present between helices in the crystalline packing. Nevertheless a part of ligand molecules is more mobile and can be released by hydrolysis leading to the formation of the more dense  $V_{6II}$  packing.

### 3.5. Stoichiometry of the different complexes studied

The different amounts of ligand determined in the total sample, after washing and acid hydrolysis are summarized in Table 3.

#### 3.5.1. Concerning the trapped molecules in amorphous and crystalline areas

Optimization of the washing procedure has consisted in finding a compromise between removing the maximum amount of free ligand and keeping the crystalline structure intact. The amount present in both the amorphous and crystalline regions was determined from the first washing treatment as described above. It represents  $7.1 \pm 1.4\%$ ,  $8.4 \pm 1.2\%$  and  $8.6 \pm 1.4\%$  (Table 3) for decanoic acid, hexanoic acid and 1,5-decanolactone, respectively. It corresponds to molar ratio ( $n_{\text{ligand}}/n_{\text{glucose}}$ ) of 0.072, 0.125 and 0.091, respectively (Table 3). These values are close to the those found by Wulff et al. (2005) between 0.040 (with (E;E)-2,4-decadienal) and 0.122 (with hexanal) and Godet et al. (1995b) between 0.063 and 0.333 for amylose–fatty acids with different chain lengths. Rutschmann et al. (1989;1990b, 1990c



determined smaller values ( $n_{\text{ligand}}/n_{\text{glucose}}$  between 0.006 and 0.062) for complexes with menthone, decanal, 1-naphthol, glycerol-1-monostearate, glycerol-1-monopalmitate and (–)limonene.

### 3.5.2. Concerning the trapped molecules in crystalline areas only

The amount of ligand determined after acid hydrolysis may be used to determine the number of ligand molecules in the crystalline parts of the complex. For the V<sub>6I</sub> crystalline packing, it corresponds closely to the amount present within the single helices, since sufficient space is not available to accommodate any molecules of ligand between helices in the unit cell. Godet et al. (1993) have proposed a model for inclusion of fatty acid in this type of amylose helix. They have shown that one CH<sub>2</sub> group of the fatty acid aliphatic chain corresponds along the helical axis to one glucose monomer. Here, the amount of decanoic acid present within the amylose helices was estimated to be  $4.5 \pm 1.4\%$  that is a molar ratio ( $n_{\text{ligand}}/n_{\text{glucose}}$ ) of 0.046 corresponding to 22 glucosyl units for one molecule of decanoic acid. If we consider that the final average DP was around 16, we have roughly one molecule of decanoic acid per helix.

For V<sub>6II</sub> and V<sub>6III</sub> crystalline packings, the ligand molecules remaining after acid hydrolysis can be trapped both within and between helices. The amount was found to be 5.6% and 7.4%, which corresponds to 1.33 and 1.22 mol of ligand per mole of amylose ( $n_{\text{ligand}}/n_{\text{amylose}}$ ) for hexanoic acid and 1,5-decanolactone, respectively (Table 3). Assuming that the mean DP is the same as for the amylose–decanoic complex and considering that there are four helices in the unit cell of V<sub>6II</sub> (Helbert & Chanzy, 1994) and V<sub>6III</sub> (Bul  on et al., 1990), the amount of ligand per unit cell would be 5.3 and 4.9 for hexanoic acid and 1,5-decanolactone, respectively. Given the poor stability of the amylose–hexanoic acid complex, the ligand is probably only included between amylose helices while the higher stability of the 1,5-decanolactone complex during hydrolysis suggests that the ligand is probably present both inside and between helices.

## 4. Conclusion

In the present study, several aroma compounds (decanoic acid, hexanoic acid and 1,5-decanolactone) were used to prepare semi-crystalline complexes with amylose. Decanoic acid induces the complexing of amylose in the V<sub>6I</sub> type, hexanoic acid in V<sub>6II</sub> and 1,5-decanolactone in V<sub>6III</sub>. The total amount of aroma compound trapped varies from 7% to 9% (w/w) as a function of the complexing molecule. It is similar to the results previously obtained with amylose fatty acids complexes or other complexes. The amount present in the crystalline parts varies from 4.5% for decanoic acid to 7.4% for 1,5-decanolactone. While decanoic acid is only present inside the amylose helix in the crystalline domains, we proposed that (i) hexanoic acid is present

between helices and (ii) 1,5-decanolactone is trapped both inside and between the helices.

Besides a more detailed knowledge of the structure and the stoichiometry of amylose complexes depending on the nature of the ligand, this work may have some applications in the field of food processing. Other flavours and aroma compounds have the ability to form inclusion complexes with amylose (Nuessli et al., 2003). Moreover, preliminary results have shown that crystallisation of amylose–aroma compounds complexes may occur in starch and real food systems (sponge cake). The conditions used in this work for complexing amylose were similar, in terms of temperature and water content, to those found in bakeries. The understanding of interactions between flavour compounds and amylose, and the knowledge of resulting structures are essential to assess both the retention and the release of aroma molecules throughout the food's lifetime (i.e., processing, cooking, aging).

## Acknowledgements

This work has been partially funded by a European network and the French ministry of research.

## References

- Arvisenet, G., Le Bail, P., Voilley, A., & Cayot, N. (2002). Influence of physicochemical interactions between amylose and aroma compounds on the retention of aroma in food-like matrices. *Journal of Agricultural and Food Chemistry*, 50(24), 7088–7093.
- Banks, W., & Greenwood, C. T. (1969). Viscosity and sedimentation studies on amylose in aqueous solution – further evidence for non-helical character. *European Polymer Journal*, 5(5), 649–658.
- Biliaderis, C. G., Page, C. M., & Maurice, T. J. (1986). Non-equilibrium melting of amylose–V complexes. *Carbohydrate Polymers*, 6, 269–288.
- Bluhm, T. L., & Zugenmaier, P. (1981). Detailed structure of the Vh-amylose–iodine complex: a linear polyiodine chain. *Carbohydrate Research*, 89(1), 1–10.
- Brisson, J., Chanzy, H., & Winter, W. T. (1991). The crystal and molecular structure of Vh amylose by electron diffraction analysis. *International Journal of Biological Macromolecules*, 13(2), 31–39.
- Bul  on, A., Delage, M. M., Brisson, J., & Chanzy, H. (1990). Single crystals of V amylose complexed with isopropanol and acetone. *International Journal of Biological Macromolecules*, 12(2), 25–33.
- Bul  on, A., Duprat, F., Booy, F. P., & Chanzy, H. (1984). Single crystals of amylose with a low degree of polymerisation. *Carbohydrate Research*, 4, 161–173.
- Cael, J. J., Koenig, J. L., & Blackwell, J. (1975). Infrared and Raman spectroscopy of carbohydrates. Part VI: normal coordinate analysis of V-amylose. *Biopolymers*, 14(9), 1885–1903.
- Fanta, G. F., Shogren, R. L., & Salch, J. H. (1999). Stream jet cooking of high-amylose starch–fatty acid mixtures. An investigation of complex formation. *Carbohydrate Polymers*, 38, 1–6.
- Galloway, G., Biliaderis, C. G., & Stanley, D. W. (1989). Properties and structure of amylose–glycerol monostearate complexes formed in solution or on extrusion of wheat flour. *Journal of Food Science*, 54, 950–957.
- Godet, M. C. (1994). M  canismes de formation des complexes Amylose–Acide gras, Ph.D Thesis, Universit   de Nantes, France.

- Godet, M. C., Bizot, H., & Buléon, A. (1995a). Crystallization of amylose–fatty acid complexes prepared with different amylose chain lengths. *Carbohydrate Polymers*, 27, 47–52.
- Godet, M. C., Bouchet, B., Colonna, P., Gallant, D. J., & Buléon, A. (1996). Crystalline amylose–fatty acid complexes: morphology and crystal thickness. *Journal of Food Science*, 61(6), 1196–1201.
- Godet, M. C., Tran, V., Colonna, P., Buléon, A., & Pezolet, M. (1995b). Inclusion/exclusion of fatty acids in amylose complexes as a function of the fatty acid chain length. *International Journal of Biological Macromolecules*, 17(6), 405–408.
- Godet, M. C., Tran, V., Delage, M. M., & Buléon, A. (1993). Molecular modelling of the specific interactions involved in the amylose complexation by fatty acids. *International Journal of Biological Macromolecules*, 15, 11–16.
- Heinemann, C., Conde-Petit, B., Nuessli, J., & Escher, F. (2001). Evidence of starch inclusion complexation with lactones. *Journal of Agricultural and Food Chemistry*, 49, 1370–1376.
- Heinemann, C., Escher, F., & Conde-Petit, B. (2003). Structural features of starch–lactone inclusion complexes in aqueous potato starch dispersions: the role of amylose and amylopectin. *Carbohydrate Polymers*, 51, 159–168.
- Helbert, W., & Chanzy, H. (1994). Single crystals of V amylose complexed with *n*-butanol or *n*-pentanol: structural features and properties. *International Journal of Biological Macromolecules*, 16(4), 207–213.
- Hermans, P. H., & Weidinger, A. (1961). On the determination of the crystalline fraction of isotactic polypropylene from X-ray diffraction. *Die Makromolekulare Chemie*, 44, 24–36.
- Hulleman, S. H. D., Helbert, W., & Chanzy, H. (1996). Single crystals of V amylose complexed with glycerol. *International Journal of Biological Macromolecules*, 18, 115–122.
- Karkalas, J., & Raphaelides, S. (1986). Quantitative aspect of amylose–lipid interactions. *Carbohydrate Research*, 157, 215–234.
- Le Bail, P., Bizot, H., Pontoire, B., & Buléon, A. (1995). Polymorphic transitions of amylose–ethanol crystalline complexes by moisture exchanges. *Starch/Stärke*, 47, 229–232.
- Le Bail, P., Rondeau, C., & Buléon, A. (2005). Structural investigation of amylose complexes with small ligands: helical conformation, crystal-line structure and thermostability. *International Journal of Biological Macromolecules*, 35, 1–7.
- Miles, M. J., Morris, V. C., Orford, P. D., & Ring, S. G. (1985). The role of amylose and amylopectin in the gelation and retrogradation of starch. *Carbohydrate Research*, 135, 271–281.
- Nelson, H. (1944). A photometric adaptation of the Somogyi method for the determination of glucose. *Journal of Biological Chemistry*, 153, 375–380.
- Nuessli, J., Putaux, J. L., Le Bail, P., & Buléon, A. (2003). Crystal structure of amylose complexes with small ligands. *International Journal of Biological Macromolecules*, 33, 227–234.
- Nuessli, J., Sigg, B., Conde-Petit, B., & Escher, F. (1997). Characterization of amylose–flavour complexes by DSC and X-ray diffraction. *Food Hydrocolloids*, 11(1), 27–34.
- Rappenecker, G., & Zugenmaier, P. (1981). Detailed refinement of the crystal structure of Vh-amylose. *Carbohydrate Research*, 89, 11–19.
- Robert, P., Devaux, M.-F., & Bertrand, D. (1996). Beyond prediction: extracting relevant information from near infrared spectra. *Journal of Near Infrared Spectroscopy*, 4, 75–84.
- Robin, J. P. (1976). Comportement du grain d'amidon à l'hydrolyse acide ménagée. Etude physico-chimique et enzymatique de la fraction insoluble. Contribution à la connaissance de la structure de l'amylopectine., PhD Thesis, Université Pierre et Marie Curie de Paris, France.
- Robin, J. P., Mercier, C., Charboniere, R., & Guilbot, A. (1974). Lintnerized starches. Gel filtration and enzymatic studies of insoluble residues from prolonged acid treatment of potato starch. *Cereal Chemistry*, 51, 389–406.
- Rutschmann, M. A., Heiniger, J., Pliska, V., & Solms, J. (1989). Formation of inclusion complexes of starch with different organic compounds. I. Method of evaluation of binding profiles with menthone as an example. *Lebensmittel-Wissenschaft und Technologie*, 22, 240–244.
- Rutschmann, M. A., & Solms, J. (1990a). Formation of inclusion complexes of starch in ternary model systems with decanal, menthone and 1-naphthol. *Lebensmittel-Wissenschaft und Technologie*, 23(5), 457–464.
- Rutschmann, M. A., & Solms, J. (1990b). Formation of inclusion complexes of starch with different organic compounds. II. Study of ligand binding in binary models systems with decanal, 1-naphthol, monostearate and monopalmitate. *Lebensmittel-Wissenschaft und Technologie*, 23, 70–79.
- Rutschmann, M. A., & Solms, J. (1990c). Formation of inclusion complexes of starch with different organic compounds. III. Study of ligand binding in binary models systems with (–)limonene. *Lebensmittel-Wissenschaft und Technologie*, 23, 80–83.
- Rutschmann, M. A., & Solms, J. (1990d). Formation of inclusion complexes of starch with different organic compounds. IV. Ligand binding and variability in helical conformations of V amylose complexes. *Lebensmittel-Wissenschaft und Technologie*, 23, 84–87.
- Sarko, A., & Biloski, A. (1980). Crystal structure of the KOH-amylose complex. *Carbohydrate Research*, 79(1), 11–21.
- Tollier, M.-T., & Robin, J. P. (1979). Adaptation de la méthode à l'orcinol-sulfurique au dosage automatique des glucides neutres totaux : conditions d'application aux extraits d'origine végétale. *Annales de technologie agricole*, 28(1), 1–15.
- Wakelin, J. H., Virgin, H. S., & Crystal, E. (1959). Development and comparison of two X-ray methods for determining the crystallinity of cotton cellulose. *Journal of Applied Physics*, 30, 1654–1662.
- Whittam, M. A., Orford, P. D., Ring, S. G., Clark, S. A., Parker, M. L., Cairns, P., & Miles, M. J. (1989). Aqueous dissolution of crystalline and amorphous amylose–alcohol complexes. *International Journal of Biological Macromolecules*, 11(12), 339–344.
- Winter, W. T., & Sarko, A. (1974). Crystal and molecular structure of the amylose–DMSO complex. *Biopolymers*, 13, 1461–1482.
- Wulff, G., Avgenaki, G., & Guzmán, M. S. P. (2005). Molecular encapsulation of flavours as helical inclusion complexes of amylose. *Journal of Cereal Science*, 41, 1–11.
- Yamashita, Y., & Monobe, K. (1971). Single crystals of amylose–V complexes. II. Crystals with 8<sub>1</sub> helical configuration. *Journal of Polymer Science*, 41, 1471–1481.
- Yu, X., Houtman, C., & Atalla, R. H. (1996). The complex of amylose and iodine. *Carbohydrate Research*, 292, 129–141.